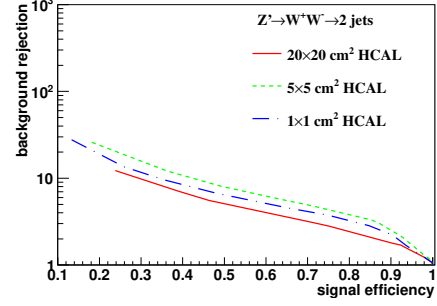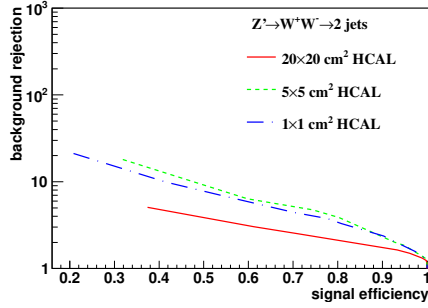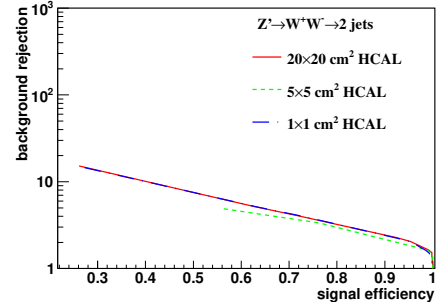(a) Z'(5 TeV)

(b) Z'(10 TeV)

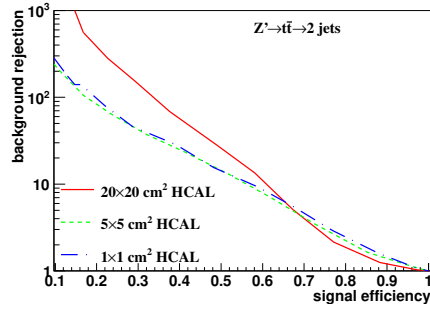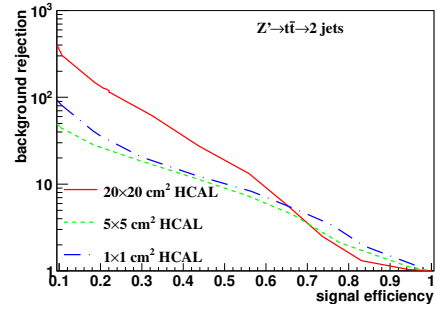(c) Z'(20 TeV)

(d) Z'(40 TeV)

Figure 1: Signal efficiency versus background rejection rate using τ_{21}. The energies of collision at (a) 5, (b) 10, (c) 20, and (d) 40 TeV are shown here. In each figure, the three ROC curves correspond to different detector sizes.

No mass cut study of detector performance with jet substructure variables

Figure 2: Signal efficiency versus background rejection rate using τ_{32}. The energies of collision at (a) 5, (b) 10, (c) 20, and (d) 40 TeV are shown here. In each figure, the three ROC curves correspond to different detector sizes.
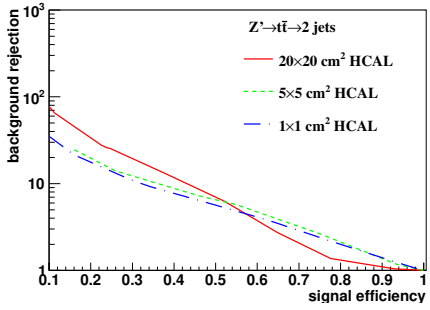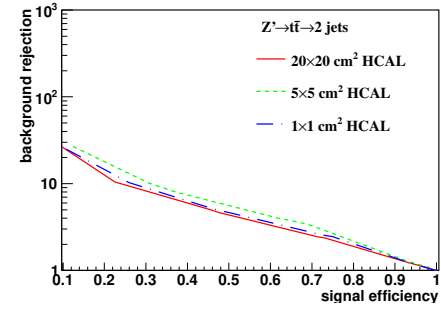
(a) Z'(5 TeV)

(b) Z'(10 TeV)
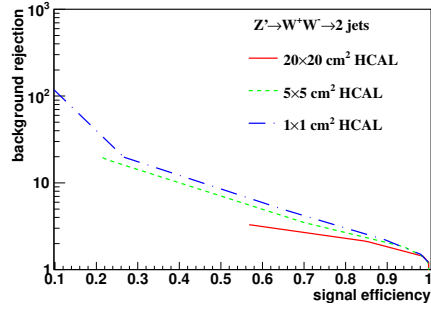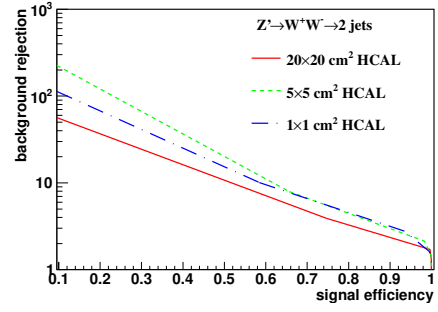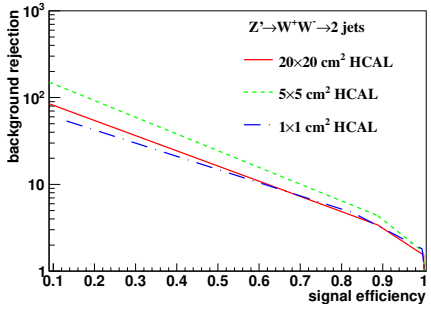

(c) Z'(20 TeV)

(d) Z'(40 TeV)

Figure 3: Signal efficiency versus background rejection rate using C_2^1. The energies of collision at (a) 5, (b) 10, (c) 20, and (d) 40 TeV are shown here. In each figure, the three ROC cu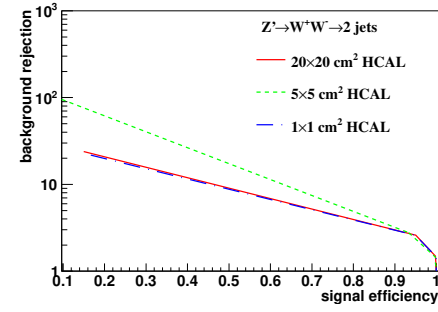rves correspond to different detector sizes.